Monthly Notices of the Royal Astronomical Society

Mon. Not. R. Astron. Soc. **415,** 3485–3496 (2011) doi:10.1111/j.1365-2966.2011.18956.x

Weak lensing reconstruction through cosmic magnification – I. A minimal variance map reconstruction

Xinjuan Yang[1,2]★ and Pengjie Zhang[3]

[1] *National Astronomical Observatories, Chinese Academy of Sciences, Beijing 100012, China*
[2] *Graduate University of Chinese Academy of Sciences, 19A, Yuquan Road, Beijing 100049, China*
[3] *Key Laboratory for Research in Galaxies and Cosmology, Shanghai Astronomical Observatory, Nandan Road 80, Shanghai 200030, China*

Accepted 2011 April 25. Received 2011 April 19; in original form 2011 March 8

ABSTRACT

We present a concept study on weak lensing map reconstruction through the cosmic magnification effect in galaxy number density distribution. We propose a minimal variance linear estimator to minimize both the dominant systematic and statistical errors in the map reconstruction. It utilizes the distinctively different flux dependences to separate the cosmic magnification signal from the overwhelming galaxy intrinsic clustering noise. It also minimizes the shot noise error by an optimal weighting scheme on the galaxy number density in each flux bin. Our method is in principle applicable to all galaxy surveys with reasonable redshift information. We demonstrate its applicability against the planned Square Kilometer Array survey, under simplified conditions. Weak lensing maps reconstructed through our method are complementary to that from cosmic shear and cosmic microwave background (CMB) and 21-cm lensing. They are useful for cross-checking over systematic errors in weak lensing reconstruction and for improving cosmological constraints.

Key words: gravitational lensing: weak – cosmology: theory – dark matter – large-scale structure of Universe.

1 INTRODUCTION

Weak gravitational lensing has been established as one of the most powerful probes of the dark Universe (Refregier 2003; Albrecht et al. 2006; Hoekstra & Jain 2008; Munshi et al. 2008). It is rich in physics and contains tremendous information on dark matter, dark energy and the nature of gravity at cosmological scales. Its modelling is relatively clean. At the multipole $\ell < 2000$, gravity is the dominant force shaping the weak lensing power spectrum while complicated gas physics only affects the lensing power spectrum at less than the 1 per cent level (White 2004; Zhan & Knox 2004; Jing et al. 2006; Rudd, Zentner & Kravtsov 2008). This makes the weak lensing precision modelling feasible, through high-precision simulations.

Precision weak lensing measurement is also promising. The most sophisticated and successful method so far is to measure the cosmic shear, lensing-induced galaxy shape distortion. After the first detections in the year 2000 (Bacon, Refregier & Ellis 2000; Kaiser, Wilson & Luppino 2000; Van Waerbeke et al. 2000; Wittman et al. 2000), data quality has been improved dramatically (e.g. Fu et al. 2008). The ongoing and planned surveys, such as DES,[1] LSST,[2] JDEM[3] and Pan-STARRS,[4] have great promise for further significant improvement.

However, weak lensing reconstruction through cosmic shear still suffers from practical difficulties associated with galaxy shape. These include shape measurement errors (additive and multiplicative) (Heymans et al. 2006; Massey et al. 2007) and the galaxy intrinsic alignment (Croft & Metzler 2000; Heavens, Refregier & Heymans 2000; Jing 2002; Hirata & Seljak 2004; Mandelbaum et al. 2006; Hirata et al. 2007; Okumura & Jing 2009; Okumura, Jing & Li 2009).

An alternative method for weak lensing reconstruction is through cosmic magnification, the lensing-induced fluctuation in galaxy (or quasar and any other celestial object) number density (Menard 2002 and references therein). Since it does not involve galaxy shape, it automatically avoids all problems associated with galaxy shape.

However, the amplitude of cosmic magnification in galaxy number density fluctuation is usually one or more orders of magnitude overwhelmed by the intrinsic galaxy number fluctuation associated with the large-scale structure of the Universe. Existing cosmic magnification measurements (Scranton et al. 2005; Hildebrandt, Waerbeke & Erben 2009; Menard et al. 2010; Van Waerbeke 2010) circumvent this problem by cross-correlating two galaxy (quasar)

★E-mail: yxj@bao.ac.cn
[1] http://www.darkenergysurvey.org
[2] http://www.lsst.org
[3] http://jdem.gsfc.nasa.gov
[4] http://pan-starrs.ifa.hawaii.edu/public/science

samples widely separated in redshift. Unfortunately, the measured galaxy–galaxy cross-correlation is often dominated by the foreground galaxy density–background cosmic magnification correlation and is hence proportional to a unknown galaxy bias of foreground galaxies. This severely limits its cosmological application.

The intrinsic galaxy clustering and cosmic magnification have a different redshift and flux dependence, which can be utilized to extract cosmic magnification. Zhang & Pen (2006) demonstrated that, by choosing (foreground and background) galaxy samples sufficiently bright and sufficiently far away, the measured cross-correlation signal can be dominated by the cosmic magnification–cosmic magnification correlation, which is free of the unknown galaxy bias. However, even for those galaxy samples, the foreground galaxy density–background cosmic magnification correlation is still non-negligible (Zhang & Pen 2006). This again limits its cosmological application due to the galaxy bias problem.

Zhang & Pen (2005) further showed that, since the galaxy intrinsic clustering and cosmic magnification have a distinctive dependence on galaxy flux, cosmic magnification can be extracted by appropriate weighting over the observed galaxy number density in each flux bin. Weak lensing reconstructed from spectroscopic redshift surveys such as the Square Kilometer Array (SKA) in this way can achieve accuracy comparable to that of cosmic shear of stage IV projects. These works demonstrate the great potential of cosmic magnification as a tool of precision weak lensing reconstruction. Furthermore, since cosmic shear and cosmic magnification are independent methods, they would provide valuable cross-checks of systematic errors in weak lensing measurements and useful information on galaxy physics such as galaxy intrinsic alignment.

Zhang & Pen (2005) only discussed two limiting cases, completely deterministic and completely stochastic biases with known flux dependence. In reality, galaxy bias could be partly stochastic. Furthermore, the flux dependence of galaxy bias is not given a priori. In this paper, we aim to investigate a key question: are we able to simultaneously measure both cosmic magnification and the intrinsic galaxy clustering, given the galaxy number density measurements in flux and redshift bins?

The paper is organized as follows. In Section 2, we present the basics of cosmic magnification and derive a minimal variance estimator for weak lensing reconstruction through cosmic magnification. In a companion paper we will discuss an alternative method to measure the lensing power spectrum through cosmic magnification. In Section 3, we discuss various statistical and systematic errors associated with this reconstruction. In Section 4, we target SKA to demonstrate the performance of the proposed estimator. We discuss and summarize in Section 5. The SKA specifications are presented in Appendix A. Throughout the paper, we adopt the *WMAP* 5-year data (Komatsu et al. 2009) with $\Omega_{\rm m} = 0.26$, $\Omega_\Lambda = 0.74$, $\Omega_{\rm b} = 0.044$, $h = 0.72$, $n_{\rm s} = 0.96$ and $\sigma_8 = 0.80$.

2 A MINIMAL VARIANCE LINEAR ESTIMATOR

Weak lensing changes the number density of background objects, which is called cosmic magnification. It involves two competing effects: a magnification of the solid angle of source objects, leading to dilution of the source number density, and a magnification of the flux, making objects brighter. Let $n(s, z_{\rm s})$ be the unlensed number density at flux s and redshift $z_{\rm s}$, and let the corresponding lensed quantity be $n^{\rm L}(s^{\rm L}, z_{\rm s})$. Throughout the paper the superscript 'L' denotes lensed quantity. The galaxy number conservation then relates the two by

$$n^{\rm L}\left(s^{\rm L}, z_{\rm s}\right) {\rm d}s^{\rm L} = \frac{1}{\mu} n(s, z_{\rm s}) {\rm d}s, \tag{1}$$

where $s^{\rm L} = s\mu$. $\mu(\boldsymbol{\theta}, z_{\rm s})$ is the lensing magnification at the corresponding direction $\boldsymbol{\theta}$ and redshift $z_{\rm s}$:

$$\mu(\boldsymbol{\theta}, z_{\rm s}) = \frac{1}{[1-\kappa(\boldsymbol{\theta}, z_{\rm s})]^2 - \gamma^2(\boldsymbol{\theta}, z_{\rm s})} \approx 1 + 2\kappa(\boldsymbol{\theta}, z_{\rm s}). \tag{2}$$

The last expression has adopted the weak lensing approximation such that the lensing convergence κ and the lensing shear γ are both much smaller than unity ($|\kappa|$, $|\gamma| \ll 1$). κ for a source at redshift $z_{\rm s}$ is related to the matter overdensity $\delta_{\rm m}$ along the line of sight by

$$\kappa(\boldsymbol{\theta}, z_{\rm s}) = \frac{3H_0^2\Omega_{\rm m}}{2c^2} \int_0^{\chi_{\rm s}} \frac{D(\chi_{\rm s}-\chi)D(\chi)}{D(\chi_{\rm s})} \delta_{\rm m}(z, \boldsymbol{\theta})(1+z) {\rm d}\chi. \tag{3}$$

Here, χ and $\chi_{\rm s}$ are the radial comoving distances to the lens at redshift z and the source at redshift $z_{\rm s}$, respectively. $D(\chi)$ denotes the comoving angular diameter distance, which equals χ for a flat universe.

Taylor expanding equation (1) around the flux $s^{\rm L}$, we obtain

$$n^{\rm L}(s^{\rm L}) = \frac{1}{\mu^2} n\left(\frac{s^{\rm L}}{\mu}\right) \approx n(s^{\rm L})[1 + 2(\alpha-1)\kappa + O(\kappa^2)], \tag{4}$$

where the parameter α is related to the logarithmic slope of the luminosity function,

$$\alpha \equiv -\frac{s^{\rm L}}{n(s^{\rm L})} \frac{{\rm d}n(s^{\rm L})}{{\rm d}s^{\rm L}} - 1 = -\frac{{\rm d}\ln n(s^{\rm L})}{{\rm d}\ln s^{\rm L}} - 1. \tag{5}$$

Note that $n(s^{\rm L})$ is related to the cumulative luminosity function $N(>s)$ by $N(>s) = \int_s^\infty n(s^{\rm L}) {\rm d}s^{\rm L}$. Weak lensing then modifies the galaxy number overdensity to

$$\delta_{\rm g}^{\rm L} \simeq \delta_{\rm g} + 2(\alpha-1)\kappa \equiv \delta_{\rm g} + g\kappa. \tag{6}$$

Here, $\delta_{\rm g}$ is the intrinsic (unlensed) galaxy number overdensity (galaxy intrinsic clustering). For brevity, we define $g \equiv 2(\alpha - 1)$ and will use this notation throughout the paper. Obviously, to the first order of gravitational lensing, the cosmic magnification effect can be totally described by the cosmic convergence and the slope of the galaxy number count.

The luminosity function averaged over a sufficiently large sky area is essentially unchanged by lensing,

$$\langle n^{\rm L}\rangle = \langle n\rangle(1 + O(\langle\kappa^2\rangle)) \approx \langle n\rangle. \tag{7}$$

The last expression is accurate to 0.1 per cent since $\langle\kappa^2\rangle \sim 10^{-3}$. The above approximation is important in cosmic magnification. It allows us to calculate α by replacing the unlensed (and hence unknown) luminosity function n with $n^{\rm L}$, the directly observed one. This means that α is also an observable and its flux dependence is directly given by observations. We will see that this is the key to extract cosmic magnification from the galaxy number density distribution.

The biggest challenge in weak lensing reconstruction through cosmic magnification is to remove the galaxy intrinsic clustering $\delta_{\rm g}$. This kind of noise in cosmic magnification measurement is analogous to the galaxy intrinsic alignment in cosmic shear measurement. But the situation here is much more severe, since $\delta_{\rm g}$ is known to be strongly correlated over a wide range of angular scales and making it overwhelming is the lensing signal at virtually all the angular scales (Figs 1 and 2).

To a good approximation, $\delta_{\rm g} = b_{\rm g}\delta_{\rm m}$, where $\delta_{\rm m}$ is defined as the matter surface overdensity and $b_{\rm g}$ is the galaxy bias. This is the

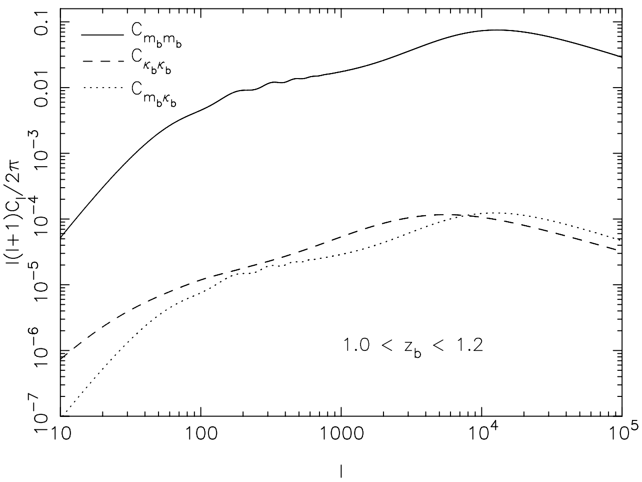

Figure 1. Contaminations of the galaxy intrinsic clustering to the weak lensing reconstruction through cosmic magnification. The dominant contamination comes from the galaxy autocorrelation, which is often several orders of magnitude larger than the lensing correlation. The galaxy intrinsic clustering also induces a galaxy–lensing cross-correlation. This contamination can be comparable to the lensing signal. For a redshift bin $1.0 < z_b < 1.2$, we plot the resulting matter power spectrum $C_{m_b m_b}$, the matter–lensing cross-power spectrum $C_{m_b\kappa_b}$ and the lensing power spectrum $C_{\kappa_b\kappa_b}$. For galaxies with bias $b_g \neq 1$, a factor b_g^2 will be applied to $C_{m_b m_b}$ and a factor b_g will be applied to $C_{m_b\kappa_b}$.

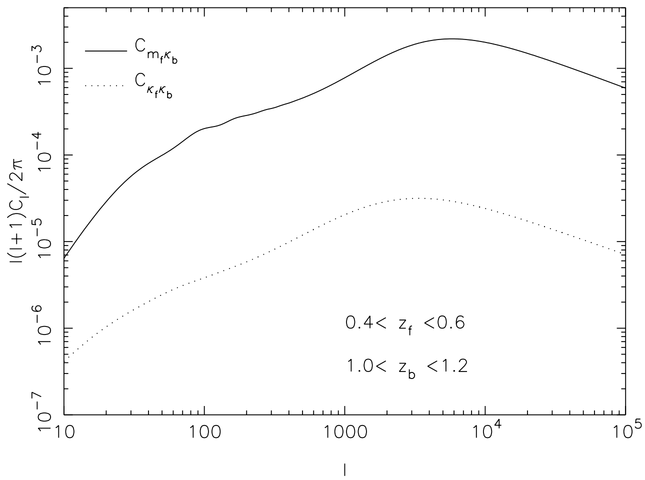

Figure 2. Contamination of foreground galaxy intrinsic clustering to the cross-correlation weak lensing power spectrum between foreground and background redshift bins. The foreground galaxy intrinsic clustering is related to the background cosmic convergence and then it induces a power spectrum $C_{m_f\kappa_b}$. We plot the weak-lensing signal $C_{\kappa_f\kappa_b}$ and the main contamination power spectrum $C_{m_f\kappa_b}$ for a couple of redshift bins ([$0.4 < z_f < 0.6$, $1.0 < z_b < 1.2$]). The contamination overwhelms the signal by one or more orders of magnitude.

limiting case of deterministic bias. In general, for statistics no higher than second order, δ_g can be described with an extra parameter, the galaxy–matter cross-correlation coefficient r. b_g and r are defined through

$$b_g^2(l,z) \equiv \frac{C_g(l,z)}{C_m(l,z)}, \qquad r(l,z) \equiv \frac{C_{gm}(l,z)}{\sqrt{C_g(l,z)C_m(l,z)}}. \tag{8}$$

Here, C_g, C_m and C_{gm} are the galaxy, matter and galaxy–matter angular power spectrum, respectively. On large scales corresponding to $l \lesssim k_L\chi$ ($k_L \sim 0.1\,h$ Mpc^{-1}), the deterministic bias ($r = 1$) is expected. However, on non-linear scales, galaxy bias is known to be stochastic (Pen 1998, 2004; Dekel & Lahav 1999; Hoekstra et al. 2002; Fan 2003; Pen et al. 2003).

2.1 The estimator

The data we have are measurements of $\delta_g^L(\boldsymbol{\theta})$ at each angular pixel of each redshift and flux bin. Throughout the paper we use the subscripts 'i' and 'j' to denote the flux bins. For convenience, we will work in Fourier space. Then for a given redshift bin and a given multipole $\boldsymbol{\ell}$, we have the Fourier transform of the galaxy overdensity of the ith flux bin, $\delta_{g,i}^L(\boldsymbol{\ell})$. For brevity, we simply denote it by δ_i^L hereafter. The g factor of the ith flux bin is denoted by g_i. As explained earlier, it is a measurable quantity. b_i is the galaxy bias of the ith flux bin.

We want to find an unbiased linear estimator of the form

$$\hat{\kappa} = \sum_i w_i \delta_i^L \tag{9}$$

such that the expectation value of $\hat{\kappa}$ is equal to the true κ of this pixel. Thus the weighting function w must satisfy the following conditions:

$$\sum_i w_i g_i = 1, \tag{10}$$

$$\sum_i w_i b_i = 0. \tag{11}$$

Since the measured δ_i^L is contaminated by shot noise $\delta_i^{\rm shot}$, we will minimize the shot noise. This corresponds to the minimization

$$\left\langle \left| \sum_i w_i \delta_i^L - \kappa \right|^2 \right\rangle = \left\langle \left| \sum_i w_i \delta_i^{\rm shot} \right|^2 \right\rangle = \sum_i \frac{w_i^2}{\bar{n}_i}. \tag{12}$$

Here, $\bar{n}_i$ is the average galaxy surface number density of the ith flux bin, a directly measurable quantity. The three sets of requirements (equations 10–12) uniquely fix the solution. Using the Lagrangian multiplier method, we find the solution to be

$$w_i = \frac{\bar{n}_i}{2}(\lambda_1 g_i + \lambda_2 b_i). \tag{13}$$

Here, the two Lagrangian multipliers $\lambda_{1,2}$ are given by

$$\lambda_1 = -\frac{2\sum \bar{n}_i b_i^2}{(\sum \bar{n}_i b_i g_i)^2 - \sum \bar{n}_i b_i^2 \sum \bar{n}_i g_i^2}\,,$$
$$\lambda_2 = \frac{2\sum \bar{n}_i b_i g_i}{(\sum \bar{n}_i b_i g_i)^2 - \sum \bar{n}_i b_i^2 \sum \bar{n}_i g_i^2}. \tag{14}$$

w_i is invariant under a flux-independent scaling in b_i. For this reason, we only need to figure out the relative flux dependence in the galaxy bias, instead of its absolute value.

Despite the neat mathematical solution above, in reality we would not know the galaxy bias a priori. So we adopt a recursive procedure to simultaneously solve b_i, w_i and hence $\hat{\kappa}$.

(i) The first step. In general, the power spectrum is dominated by the galaxy intrinsic clustering, namely

$$\left\langle \left|\delta_i^L\right|^2 \right\rangle = b_i^2 C_{m_b m_b} + g_i g_i C_{\kappa_b\kappa_b} + 2 b_i g_i C_{m_b\kappa_b} \simeq b_i^2 C_{m_b m_b}. \tag{15}$$

Here, $C_{m_b m_b}$ is the matter density angular power spectrum, $C_{\kappa_b\kappa_b}$ is the lensing power spectrum and $C_{m_b\kappa_b}$ is the cross-power spectrum, all for the background redshift bin. Hence a natural initial guess for

b_i is given by the following equation:

$$\left(b_i^{(1)}\right)^2 C_{\mathrm{m_b m_b}} = \left\langle \left|\delta_i^{\mathrm{L}}\right|^2 \right\rangle. \tag{16}$$

By plugging $b_i^{(1)}$ into equations (14) and (13), we obtain the weighting $w_i^{(1)}$, and then the first guess of lensing convergence, $\kappa^{(1)} = \sum_i w_i^{(1)} \delta_i^{\mathrm{L}}$.

$C_{\mathrm{m_b m_b}}$ is cosmology-dependent, so one may think that the bias reconstruction and hence the proposed lensing reconstruction are cosmology-dependent. However, this is not the case. As explained earlier, the weighting function w_i does not depend on the absolute value of b_i. So in the exercise, $C_{\mathrm{m_b m_b}}$ can be fixed to any value of convenience in determining the bias since it is independent of flux. In this sense, the bias reconstruction is cosmology-independent and is hence free of uncertainties from cosmological parameters.

(ii) The second step. We subtract the lensing contribution from δ_i^{L}, using $\kappa^{(1)}$ constructed above. Our second guess for b_i is then

$$b_i^{(2)} b_i^{(2)} C_{\mathrm{m_b m_b}} = \left\langle \left|\delta_i^{\mathrm{L}} - g_i \kappa^{(1)}\right|^2 \right\rangle. \tag{17}$$

We then obtain $w_i^{(2)}$ and $\kappa^{(2)}$. However, this solution is still not exact. The expectation value of the right-hand side is

$$\left\langle \left|\delta_i^{\mathrm{L}} - g_i \kappa^{(1)}\right|^2 \right\rangle = \left(b_i - g_i \sum_j w_j^{(1)} b_j\right)^2 C_{\mathrm{m_b m_b}}. \tag{18}$$

So the expectation value of $b_i^{(2)}$ is $b_i - g_i \sum_j w_j^{(1)} b_j$.

(iii) The iteration. We repeat the above step to obtain $b_i^{(p)}$ and $\kappa^{(p)}$ ($p = 3, \ldots$) until the iteration converges. Since we know that the lensing contribution is subdominant and we start our iteration by ignoring the lensing contribution, and since the flux dependence of the intrinsic clustering and cosmic magnification (b_i and g_i) are different, such an iteration should be stable and should converge. We numerically check it to be the case.

The information of galaxy bias is not only encoded in the observed power spectrum of the same flux bin, but it is also encoded in the cross-power spectra between different flux bins. In our exercise, we do not take this extra information into account. So there are possibilities of further improvement.

In the above description, we have ignored shot noise (or equivalently assumed that it can be subtracted completely). In reality, we are only able to subtract shot noise up to the limit of cosmic variance. Residual shot noise introduces systematic error in the lensing reconstruction, which we will quantify in the next section.

Finally, we obtain the optimal estimator of cosmic convergence:

$$\kappa^{(n)} = \sum_i w_i^{(n)} \delta_i^{\mathrm{L}} = \kappa + \left(\sum_i w_i^{(n)} b_i\right) \delta_{\mathrm{m}}. \tag{19}$$

Our estimator explicitly satisfies $\sum_i w_i^{(n)} b_i^{(n)} = 0$. However, since $b_i^{(n)}$ can deviate from its real value b_i, our estimator can be biased. This is yet another source of systematic errors in our weak lensing reconstruction through cosmic magnification. However, later we will show that such a systematic error could be controlled.

2.2 The reconstructed weak lensing power spectrum

From the reconstructed κ, we can reconstruct the lensing power spectrum. For the same redshift bin, we have

$$\begin{aligned} C_{\mathrm{bb}} &= \left\langle |\kappa_{\mathrm{b}}^{(n)}|^2 \right\rangle \\ &= C_{\kappa_{\mathrm{b}}\kappa_{\mathrm{b}}} + \left(\sum_i w_i^{\mathrm{b}} b_i^{\mathrm{b}}\right)^2 C_{\mathrm{m_b m_b}} + 2\left(\sum_i w_i^{\mathrm{b}} b_i^{\mathrm{b}}\right) C_{\mathrm{m_b}\kappa_{\mathrm{b}}}. \end{aligned} \tag{20}$$

Throughout the paper we use the superscript or subscript 'b' for quantities of background redshift bin and 'f' for quantities of foreground redshift bin, and we ignore the superscript '(n)' of weighting $w_i^{(n)}$ from this section. For the cross-correlation between foreground and background populations, we have

$$C_{\mathrm{bf}} = \left\langle \kappa_{\mathrm{b}}^{(n)} \kappa_{\mathrm{f}}^{(n)*} \right\rangle = C_{\kappa_{\mathrm{f}}\kappa_{\mathrm{b}}} + \left(\sum_i w_i^{\mathrm{f}} b_i^{\mathrm{f}}\right) C_{\mathrm{m_f}\kappa_{\mathrm{b}}}. \tag{21}$$

Here, $C_{\kappa_{\mathrm{f}}\kappa_{\mathrm{b}}}$ is the lensing power spectrum between foreground and background redshift bins, and $C_{\mathrm{m_f}\kappa_{\mathrm{b}}}$ is the cross-power spectrum between foreground dark matter and background lensing convergence. We have ignored the correlation $C_{\mathrm{m_f m_b}}$ between foreground and background matter distributions; ignoring it is expected for non-adjacent redshift bins with separation $\Delta z \geq 0.1$, because of physical irrelevance. For two adjacent redshift bins, there is indeed a non-vanishing matter correlation. However, this correlation is also safely ignored since both the foreground and background intrinsic clusterings are sharply suppressed by factors $1/\sum_i w_i^{\mathrm{f,b}} b_i^{\mathrm{f,b}}$, respectively.

3 STATISTICAL AND SYSTEMATIC ERRORS

Our reconstruction method does not rely on priors on galaxy bias; in this sense, it is robust. However, there are still a number of statistical and systematic errors in the κ reconstruction and weak lensing power spectrum reconstruction. In this section, we outline and quantify the associated errors in the lensing power spectrum.

3.1 The statistical error

Our estimator minimizes the shot noise in the measurement. For auto-power spectrum C_{bb}, the associated statistic measurement error is

$$\begin{aligned} \Delta C_{\mathrm{bb}} &= \sqrt{\frac{1}{(2l+1)\Delta l f_{\mathrm{sky}}}} \left\langle \left(\sum_i w_i^{\mathrm{b}} \delta_i^{\mathrm{L}} - \kappa_{\mathrm{b}}\right)^2 \right\rangle \\ &= \sqrt{\frac{1}{(2l+1)\Delta l f_{\mathrm{sky}}}} \sum_i \frac{(w_i^{\mathrm{b}})^2}{\bar{n}_i^{\mathrm{b}}}. \end{aligned} \tag{22}$$

For the cross-power spectrum C_{bf}, the statistical error is

$$\begin{aligned} \Delta C_{\mathrm{bf}} &= \sqrt{\frac{1}{(2l+1)\Delta l f_{\mathrm{sky}}}} \sqrt{C_{\mathrm{b}}^{\mathrm{shot}} C_{\mathrm{f}}^{\mathrm{shot}}} \\ &= \sqrt{\frac{1}{(2l+1)\Delta l f_{\mathrm{sky}}}} \sqrt{\left(\sum_i \frac{(w_i^{\mathrm{b}})^2}{\bar{n}_i^{\mathrm{b}}}\right)\left(\sum_i \frac{(w_i^{\mathrm{f}})^2}{\bar{n}_i^{\mathrm{f}}}\right)}. \end{aligned} \tag{23}$$

Throughout the paper we apply $\Delta l = 0.2l$, and f_{sky} is the sky coverage.

The above errors are purely statistical errors caused by shot noise resulting from a sparse galaxy distribution. For this reason, we call them the weighted shot noise. We reconstruct the κ from the measurements of lensed galaxy number overdensity δ_i^{L}. We solve the galaxy bias and weighting function from the observed galaxy power spectra $\langle|\delta_i^{\mathrm{L}}|^2\rangle$ and the whole process is free of any given cosmological model. So our proposed method to reconstruct the weak lensing map is the one at the given sky coverage, with the right cosmic variance. Only when we compare our measured lensing power spectra with their ensemble average predicted by a given theory do we have to add cosmic variance. Since statistical errors arising from cosmic variance are independent of shot noise, it can be taken into account straightforwardly.

3.2 Systematic errors

We use the symbol δC to denote systematic errors in the lensing power spectrum measurement. We have identified three types of major systematic errors. Throughout the paper we use the superscript '(o)' ($o = 1, 2, 3, \ldots$) to denote them.

3.2.1 The systematic error from deterministic bias

The first set of systematic errors comes from errors in determining the galaxy bias b_i through equation (15), even if we ignore the shot noise contribution to it. This bias arises due to a degeneracy among the power spectra $C_{\mathrm{m_b m_b}}$, $C_{\mathrm{m_b}\kappa_\mathrm{b}}$, $C_{\kappa_\mathrm{b}\kappa_\mathrm{b}}$ and galaxy bias b_i in equation (15), which causes a slight deviation from its true flux dependence. In a companion paper we will address and clarify this issue in more detail (Yang & Zhang, in preparation). We will also show that this systematic error is correctable.

The consequence is that $\sum_i w_i^{(n)} b_i \neq 0$ in equation (19). It causes a systematic error in the autocorrelation of the same redshift bin:

$$\delta C_{\mathrm{bb}}^{(1)} = \left(\sum_i w_i^{\mathrm{b}} b_i^{\mathrm{b}}\right)^2 C_{\mathrm{m_b m_b}} + 2\left(\sum_i w_i^{\mathrm{b}} b_i^{\mathrm{b}}\right) C_{\mathrm{m_b}\kappa_\mathrm{b}}. \tag{24}$$

It also biases the cross-correlation measurement between two different redshift bins:

$$\delta C_{\mathrm{bf}}^{(1)} = \left(\sum_i w_i^{\mathrm{f}} b_i^{\mathrm{f}}\right) C_{\mathrm{m_f}\kappa_\mathrm{b}}. \tag{25}$$

3.2.2 The systematic error from stochastic bias

Our reconstruction has approximated the galaxy bias to be deterministic, namely $r_{ij} = 1$. r_{ij} are the correlation coefficients between galaxies with different fluxes. It is known that galaxy bias is a stochastic component and hence $r_{ij} < 1$, especially at non-linear scales (Wang et al. 2007; Swanson et al. 2008; Gil-Marin et al. 2010). This does not affect the determination of the galaxy bias b_i, since we only use the autocorrelation between the same flux and redshift bin to determine the bias. However, stochasticity does bias the power spectrum measurement, since now the condition (equation 11) no longer guarantees a complete removal of the galaxy intrinsic clustering. The systematic error induced into the autocorrelation measurement is

$$\delta C_{\mathrm{bb}}^{(2)} = -\left[\sum_{i,j} w_i^{\mathrm{b}} w_j^{\mathrm{b}} b_i^{\mathrm{b}} b_j^{\mathrm{b}} \Delta r_{ij}\right] C_{\mathrm{m_b m_b}}. \tag{26}$$

Here, $\Delta r_{ij} \equiv 1 - r_{ij}$.

Given the present poor understanding of galaxy stochasticity, we demonstrate this bias by adopting a very simple toy model, with

$$\Delta r_{ij} = 1 - r_{ij} = \begin{cases} 0 & (i = j) \\ 1\ \text{per cent} & (i \neq j). \end{cases} \tag{27}$$

This model is by no means realistic. The particular reason to choose this toy model is that readers can conveniently scale the resulting $\delta C^{(2)}$ to their favourite models of galaxy stochasticity by multiplying by the factor $100\Delta r_{ij}(\ell, z)$.

As we will show later, this systematic error could become the dominant error source. However, one can avoid this problem by measuring the lensing power spectrum between two redshift bins. Clearly, stochasticity in galaxy distribution does not bias such a cross-power spectrum measurement.

3.2.3 The systematic error from shot noise

So far we have ignored the influence of galaxy shot noise in determining the galaxy bias (equation 15). The induced error is denoted by $\delta b_j = b_j^{\mathrm{r}} - \hat{b}_j$. Here, b_j^{r} is the true bias and $\hat{b}_j$ is the final obtained bias $b_j^{(n)}$ from the iteration. It is reasonable to consider the case that shot noise is subdominant to the galaxy intrinsic clustering. Under this limit,

$$\langle \delta b_j \rangle = 0, \quad \langle (\delta b_j)^2 \rangle \simeq \frac{C_j^{\mathrm{shot}}}{C_{\mathrm{m_b m_b}}}, \tag{28}$$

where C_j^{shot} is the shot noise power spectrum of the jth flux bin in the observed power spectrum (equation 15). We are then able to Taylor expand flux weighting w_i around $\hat{b}_j$ to estimate the induced bias in it:

$$w_i(\hat{b_j} + \delta b_j) = w_i(\hat{b_j}) + \sum_j \left.\frac{\partial w_i}{\partial b_j}\right|_{\hat{b_j}} \delta b_j + \frac{1}{2}\sum_{jk} \left.\frac{\partial^2 w_i}{\partial b_j \partial b_k}\right|_{\hat{b_j}} \delta b_j \delta b_k + \cdots \tag{29}$$

where $w_i(\hat{b_j})$ is the final obtained flux weighting. After a lengthy but straightforward derivation, we derived the induced bias in the autocorrelation measurement:

$$\begin{aligned}\delta C_{\mathrm{bb}}^{(3)} = C_{\mathrm{m_b m_b}} \times \Bigg[&\sum_j \left\langle \left(\delta b_j^{\mathrm{b}}\right)^2 \right\rangle \left(\sum_i \frac{\partial w_i^{\mathrm{b}}}{\partial b_j^{\mathrm{b}}} b_i^{\mathrm{b}}\right)^2 \\ &+ \left(\sum_i w_i^{\mathrm{b}} b_i^{\mathrm{b}}\right)\left(\sum_j \left\langle \left(\delta b_j^{\mathrm{b}}\right)^2 \right\rangle \sum_i \frac{\partial^2 w_i^{\mathrm{b}}}{\partial b_j^{\mathrm{b}} \partial b_j^{\mathrm{b}}} b_i^{\mathrm{b}}\right) \\ &- \sum_k \left\langle \left(\delta b_k^{\mathrm{b}}\right)^2 \right\rangle \sum_{ij} \frac{\partial w_i^{\mathrm{b}}}{\partial b_k^{\mathrm{b}}} \frac{\partial w_j^{\mathrm{b}}}{\partial b_k^{\mathrm{b}}} b_i^{\mathrm{b}} b_j^{\mathrm{b}} \Delta r_{ij}\Bigg] \\ &+ C_{\mathrm{m_b}\kappa_\mathrm{b}} \times \left[\sum_j \left\langle \left(\delta b_j^{\mathrm{b}}\right)^2 \right\rangle \sum_i \frac{\partial^2 w_i^{\mathrm{b}}}{\partial b_j^{\mathrm{b}} \partial b_j^{\mathrm{b}}} b_i^{\mathrm{b}}\right].\end{aligned} \tag{30}$$

The induced bias in cross-correlation measurement is

$$\delta C_{\mathrm{bf}}^{(3)} = \frac{1}{2} C_{\mathrm{m_f}\kappa_\mathrm{b}} \times \left[\sum_j \left\langle \left(\delta b_j^{\mathrm{f}}\right)^2 \right\rangle \sum_i \frac{\partial^2 w_i^{\mathrm{f}}}{\partial b_j^{\mathrm{f}} \partial b_j^{\mathrm{f}}} b_i^{\mathrm{f}}\right]. \tag{31}$$

3.3 Other sources of error

There are other sources of error that we will ignore in the simplified treatment presented here. First of all, we only deal with idealized surveys with a uniform survey depth without any masks. Complexities in real surveys will not only impact the estimation of errors listed in the previous sections, but may also induce new sources of error. These errors can be investigated with a mock catalogue mimicking real observations. We defer such investigations to elsewhere.

Another source of error is the determination of α (or equivalently g). For SKA, which we will be targeting, errors in α are negligible since the galaxy luminosity function can be determined to a high accuracy given the billions of SKA galaxies with spectroscopic redshifts. However, this may not be the case for other surveys, due to at least two reasons. (1) Some surveys may not have sufficient galaxies at the bright end. Large Poisson fluctuations then forbid precision measurement of α there. (2) α is defined with respect to the galaxy luminosity function in a given redshift bin. However, a large fraction of galaxy surveys may only have the photometric redshift measurement. Errors in redshift, especially the catastrophic photo-z error, affect the measurement of α.

Dust extinction is also a problem for optical surveys, but not for radio surveys like SKA. Dust extinction also induces fluctuations into galaxy number density, with a characteristic flux dependence α. This flux dependence differs from the $\alpha - 1$ dependence in cosmic magnification and $b_g(s)$ dependence in galaxy bias. The minimal variance estimator can be modified such that $\sum_i w_i \alpha_i = 0$ to eliminate this potential source of error, when necessary.

In the next section, we will quantify the statistical and systematic errors listed in Sections 3.1 and 3.2 for the planned 21-cm survey SKA. Although the estimation is done under very simplified conditions, it nevertheless demonstrates that these errors are likely under control.

4 THE PERFORMANCE OF THE MINIMAL VARIANCE ESTIMATOR

We target SKA to investigate the feasibility of our proposal. SKA is able to detect billions of galaxies through their neutral hydrogen 21-cm emission. The survey specifications are adopted as field of view (FOV) = 10 deg^2, total survey period $t_{\rm all} = 5$ yr and total sky coverage 10^4 deg^2 (Dewdney et al. 2009; Abdalla, Blake & Rawlings 2010; Faulkner et al. 2010). More details of the survey are given in Appendix A.

Figs 1 and 2 demonstrate contaminations of galaxy intrinsic clustering to the cosmic magnification measurement from one redshift bin and one pair of foreground and background redshift bins. For a typical redshift bin $1.0 < z_{\rm b} < 1.2$, the auto matter angular power spectrum $C_{\rm m_b m_b}$ is larger than the lensing power spectrum by two or more orders of magnitude. Fig. 1 also shows that $C_{\rm m_b \kappa_b}$ is comparable to $C_{\kappa_b \kappa_b}$. Since the typical bias of 21-cm galaxies is $\sim$1 (Fig. 3), this means that the galaxy intrinsic clustering overwhelms the lensing signal by orders of magnitude. Similarly, in Fig. 2 the cross-power spectrum $C_{\rm m_f \kappa_b}$ induced by the foreground intrinsic clustering overwhelms the weak lensing power spectrum $C_{\kappa_f \kappa_b}$ by

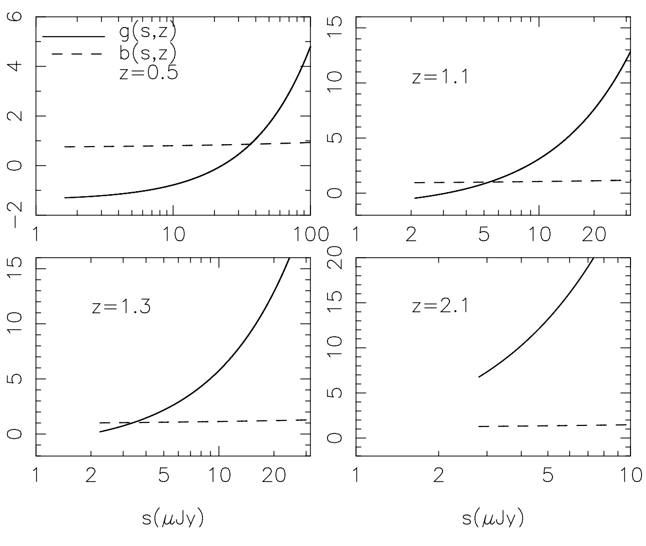

Figure 3. The H I galaxy bias $b(s, z)$ and the magnification bias $g(s, z) = 2(\alpha - 1)$ as a function of flux s by fixing the redshift to be the central value of each redshift bin. The plotted curves are started from the flux limit at the fixed redshift. The cosmic magnification bias strongly depends on the flux, while the galaxy bias weakly changes with it. Such a difference in flux dependence ensures the finding of an optimal estimator to reconstruct the weak lensing from the cosmic magnification.

one or more orders of magnitude. These big contaminations related to galaxy intrinsic clustering make the weak lensing measurement difficult from the direct cosmic magnification measurement, unless for sufficiently bright foreground and background galaxies at sufficiently high redshifts (Zhang & Pen 2006).

As we explained in earlier sections, the key to extracting the lensing signal from the overwhelming noise is the different dependences of signal and noise on the galaxy flux. Fig. 3 shows that the lensing signal and the intrinsic clustering indeed have very different dependences on the galaxy flux. For the 21-cm emitting galaxies, the flux dependence in $g \equiv 2(\alpha - 1)$ is much stronger than that in the galaxy bias. Furthermore, g changes sign from the faint end to the bright end. Such a behaviour cannot be mimicked by bias, which keeps positive.

From such a difference in the flux dependences, we expect our estimator to significantly reduce contaminations from the galaxy intrinsic clustering. As explained earlier, in the galaxy correlation between the same redshift bin, the intrinsic clustering induces a systematic error proportional to $C_{\rm m_b m_b}$ (equation 24) and an error proportional to $C_{\rm m_b \kappa_b}$ (equation 24). In the ideal case that both the stochasticity and shot noise in the galaxy distribution can be ignored, the systematic error proportional to $C_{\rm m_b m_b}$ will be suppressed by a factor $1/(\sum_i w_i^{\rm b} b_i^{\rm b})^2$ (equation 24). Fig. 4 shows that this suppression factor is of the order of $\sim 10^4$ at interesting scales $10 \lesssim \ell \lesssim 10^4$. For the same reason, the systematic error proportional to $C_{\rm m_b \kappa_b}$ will be suppressed by a factor $1/\sum_i w_i^{\rm b} b_i^{\rm b} \sim 10^2$ over the same angular scales. The systematic error induced by the foreground intrinsic clustering in the weak lensing reconstruction between two redshift bins is proportional to $C_{\rm m_f \kappa_b}$ (equation 25). Our estimator also suppresses it by a factor $1/\sum_i w_i^{\rm f} b_i^{\rm f} \sim 10^2$, as shown in Fig. 5.

4.1 Same redshift bins

The lensing power spectrum can then be directly measured through the reconstructed lensing maps. This can be done for maps of the same redshift bin. Fig. 6 compares the residual systematical errors to the lensing power spectrum signal. Overall, our minimal variance estimator significantly suppresses the galaxy intrinsic clustering and makes the weak lensing reconstruction feasible. For the source redshift $z_{\rm b} \sim 1$ (e.g. $1.0 < z_{\rm b} < 1.4$), all the investigated systematic errors and statistical errors are suppressed to be subdominant to the signal. We expect the lensing power spectrum to be measured with an accuracy of $\sim$10–20 per cent.

However, at lower and higher redshifts, the reconstruction is not successful. We observe that the systematic error $\delta C^{(1)}_{\rm bb}$ increases with increasing redshift and overwhelms the lensing signal at $z_{\rm b} \gtrsim 2$. In the current formalism it is difficult to explain this behaviour straightforwardly. But roughly speaking, this is caused by a worse initial guess on the flux dependence of galaxy bias coupled with the degeneracy explained earlier. The initial guess is accurate to the level of $C_{\kappa_b \kappa_b}/C_{\rm m_b m_b}$. So the associated error increases with redshift.

This systematic error looks rather frustrating. However, we will show that the systematic error $\delta C^{(1)}$ is correctable in the companion paper (Yang & Zhang, in preparation). In there we can separate the degeneracy, and reconstruct a quantity $y_i^{\rm b} = \sqrt{C_{\rm m_b m_b}}(b_i^{\rm b} + g_i^{\rm b} C_{\rm m_b \kappa_b}/C_{\rm m_b m_b})$ through a direct multiparameter fitting against the measured power spectra, which perfectly mimics the flux dependence of galaxy bias $b_i^{\rm b}$, because the power spectrum $C_{\rm m_b m_b}$ is independent of flux and the correction term $C_{\rm m_b \kappa_b}/C_{\rm m_b m_b}$ is small especially for high redshift. Although it is bad to find that the final convergence depends on the initial guess of galaxy bias,

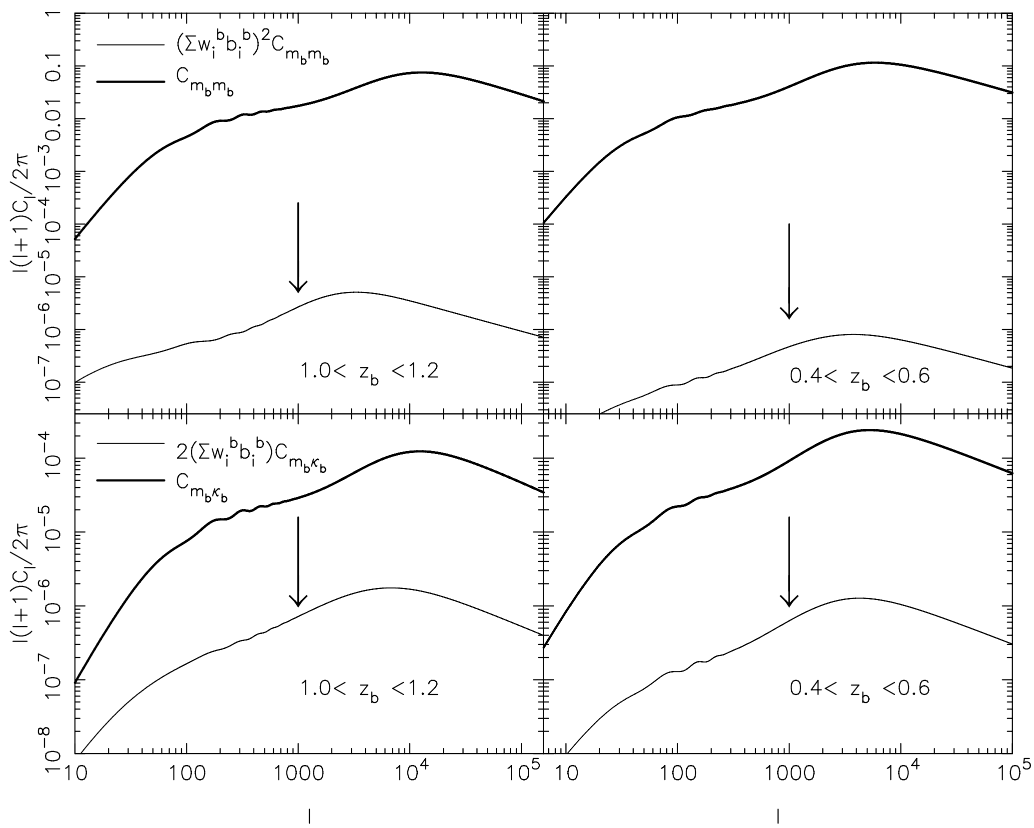

Figure 4. The contaminations before and after using the estimator to reconstruct the weak lensing auto power spectrum. We choose two redshift bins $0.4 < z_b < 0.6$ and $1.0 < z_b < 1.2$. For these bins, the upper panel shows us the suppression of matter auto power spectrum, and the lower panel presents the suppression of matter–lensing cross-power spectrum, respectively. Clearly, for the same redshift bin our reconstruction method can sharply reduce the two correlations both induced by the intrinsic clustering. The power spectrum $C_{m_b m_b}$ can be suppressed by an order of $\sim 10^4$ and the power spectrum $C_{m_b \kappa_b}$ can be reduced by one or more orders of magnitude. For the lower redshift bin, the suppression is stronger, since the value of $\sum_i w_i^b b_i^b$ rises with redshift. Roughly speaking, this results from the increasing error in the final galaxy bias. With the increasing redshift, the contribution from the weak lensing power spectrum to the observed power spectrum increases, so the error in the initial galaxy bias increases and then leads to the rising error in the final galaxy bias because of the existing degeneracy in the process of solving galaxy bias.

y_i^b as a guess of galaxy bias does reduce the systematic error $\delta C^{(1)}$ and then works far better than the galaxy bias obtained in this paper.

The systematic error $\delta C^{(3)}$ arising from shot noise becomes non-negligible at $z_b \sim 2$, due to sharply decreasing galaxy density and increasing shot noise at these redshifts (see Fig. A2). We find that this error is always subdominant to either $\delta C_{bb}^{(1)}$ or $\delta C_{bb}^{(2)}$. Interestingly, both $\delta C_{bb}^{(3)}$ and the weighted shot noise ΔC_{bb} (statistical error, equation 22) have similar shapes at all redshifts. Furthermore, both roughly scale as l^0 at low redshifts. These are not coincidences.

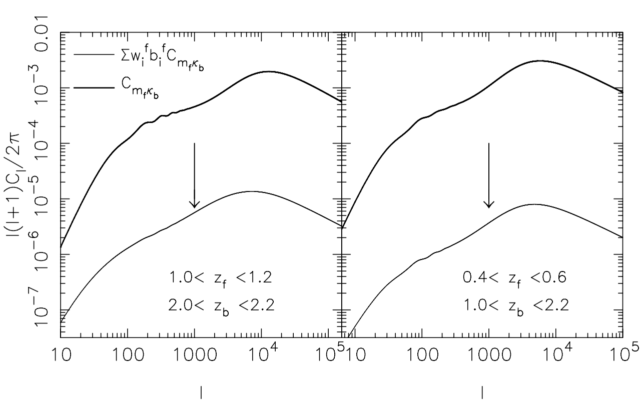

Figure 5. The suppression of contamination related with foreground intrinsic clustering in the reconstructed lensing cross-correlation power spectrum between foreground redshift bin z_f and background redshift bin z_b. Because of the reduced foreground intrinsic clustering, the enormous correction $C_{m_f \kappa_b}$ to the signal can be suppressed by a factor of $\sim 10^2$.

(i) The term $\propto C_{m_b m_b}$ is dominant in $\delta C_{bb}^{(3)}$. This term is also $\propto \langle (\delta b_j^b)^2 \rangle \propto 1/C_{m_b m_b}/\bar{n}_j$. So both $\delta C_{bb}^{(3)}$ and ΔC_{bb} are the sums of $1/\bar{n}_j$ weighted in different ways and hence have similar shapes.

(ii) The galaxy bias in our fiducial model is scale-independent. This results in a scale-independent weighting function w_j, as long the bias can be determined to high accuracy. For these reasons, $\delta C_{bb}^{(3)}$, $\Delta C_{bb} \propto l^0$. This is the case at low redshift.

(iii) However, the accuracy in determining galaxy bias is significantly degraded by contamination proportional to $C_{\kappa_b \kappa_b}/C_{m_b m_b}$, which is scale-dependent and increases with redshift. This is the reason that both $\delta C_{bb}^{(3)}$ and ΔC_{bb} show complicated angular dependence at $z_b \simeq 2$ (Fig. 6).

At low redshift (e.g. $0.4 < z_b < 0.6$), the systematic error $\delta C_{bb}^{(2)}$ arising from galaxy bias stochasticity becomes dominant or even exceeds the lensing signal. This is what is expected. The galaxy intrinsic clustering is stronger at lower redshift. This amplifies the impact of galaxy stochasticity. A weaker lensing signal at lower

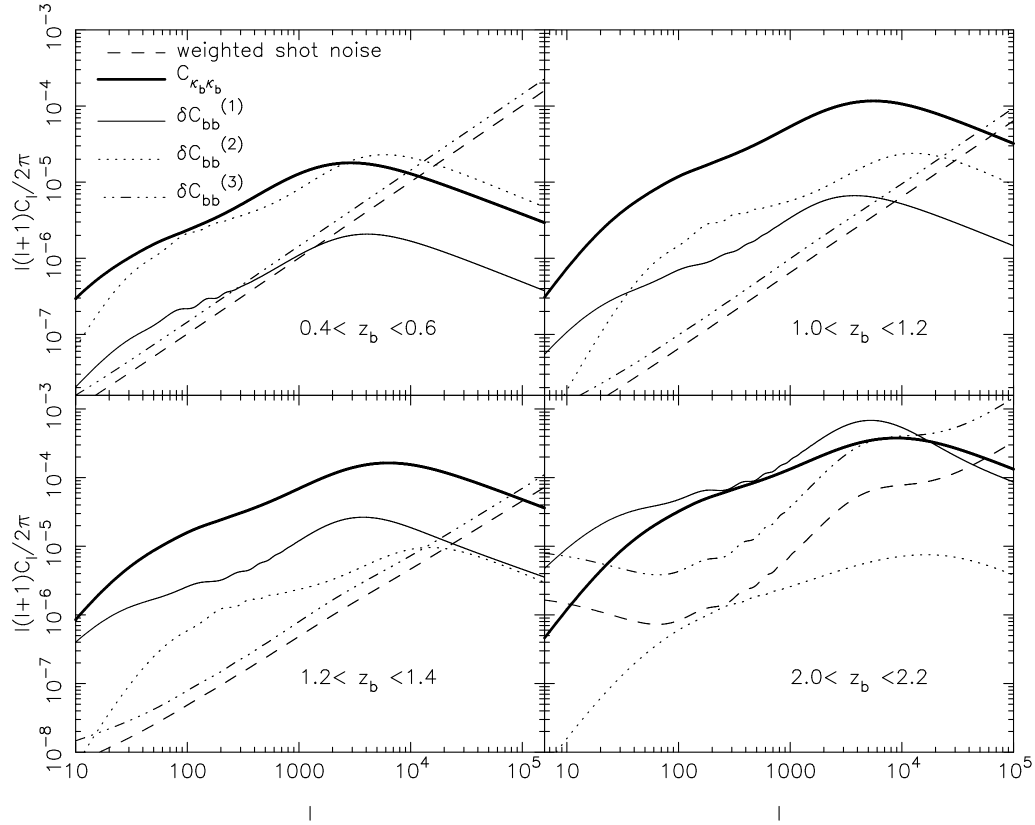

Figure 6. Composition of the reconstructed weak lensing power spectrum for the same redshift bin. We plot the weak lensing power spectrum $C_{\kappa_b\kappa_b}$ with a bold solid line. The three types of systematic errors, $\delta C^{(1)}_{bb}$ from error in deterministic galaxy bias, $\delta C^{(2)}_{bb}$ from the stochastic bias and $\delta C^{(3)}_{bb}$ from the shot noise are presented by the solid, dotted and dash-dot-dot-dotted lines, respectively. The statistical error is plotted by the dashed line. Here the statistical error is called weighted shot noise only from the sparse galaxy distribution, since we aim to reconstruct the weak lensing at each angular pixel with the corresponding cosmic variance. For the intermediate redshift bins $1.0 < z_b < 1.2$ and $1.2 < z_b < 1.4$, the signal overwhelms all these errors and can be measured to reach the ∼10–20 per cent level.

redshift further amplifies its relative impact. As expected, Fig. 6 shows that $\delta C^{(2)}_{bb}/C_{\kappa_b\kappa_b}$ decreases with increasing redshift and becomes negligible at $z_b \sim 2$. Since $\delta C^{(2)}_{bb} \propto \Delta r_{ij}$, the importance of $\delta C^{(2)}_{bb}$ is sensitive to the true nature of galaxy stochasticity. Its value should be multiplied by a factor $100\Delta r_{ij}$ for the fiducial value of $\Delta r_{ij} \neq 1$ per cent. We hence conclude that galaxy stochasticity is the likely dominant source of error in weak lensing reconstruction through cosmic magnification.

4.2 Different redshift bins

Fortunately this stochasticity issue can be safely overcome in the lensing power spectrum measurement through lensing maps reconstructed in two different redshift bins (foreground and background bins). The results are shown in Fig. 7. In this case, the systematic error is dominated by $\delta C^{(1)}_{bf}$. The stochasticity does not induce systematic error so that $\delta C^{(2)}_{bf} = 0$.

Overall, the lensing power spectrum measurement through cross-correlating reconstructed maps of different redshift bins is more robust than the one based on the same redshift bin. The reconstruction accuracy can be controlled to 10–20 per cent over a wide range of foreground and background redshifts.

At last, for a consistency test, we check whether our results depend on the division of the flux bin. As expected, various systematic errors and statistical error change little with respect to different choices of flux bins, as long as these bins are fine enough.

4.3 Uncertainties in the forecast

There are a number of uncertainties in the forecast, besides the ones discussed in the previous sections.

(i) In the fiducial galaxy intrinsic clustering model, we have ignored the scale dependence in galaxy bias.

(ii) We have ignored cosmic variance in the lensing signal so the fiducial power spectrum is the ensemble average. Fortunately, the ignored cosmic variance of each power spectrum is much smaller than the ensemble average because $l\Delta l f_{sky} \gg 1$ with a given large sky coverage of SKA ($f_{sky} = 10^4\,\mathrm{deg}^2$). Thus it is not a dominant source of error and therefore can be safely ignored at most relevant scales.

(iii) The toy model of galaxy stochasticity is too simplified. In reality, the cross-correlation coefficient r should be a function of redshift, angular scale and galaxy type and flux.

For these reasons, the numerical results presented in this paper should only be trusted as a rough estimation. A robust evaluation of the weak lensing reconstruction performance through cosmic magnification requires a much more comprehensive investigation. Nevertheless, the concept study presented in this paper demonstrates that weak lensing reconstruction through cosmic magnification is indeed a promising concept.

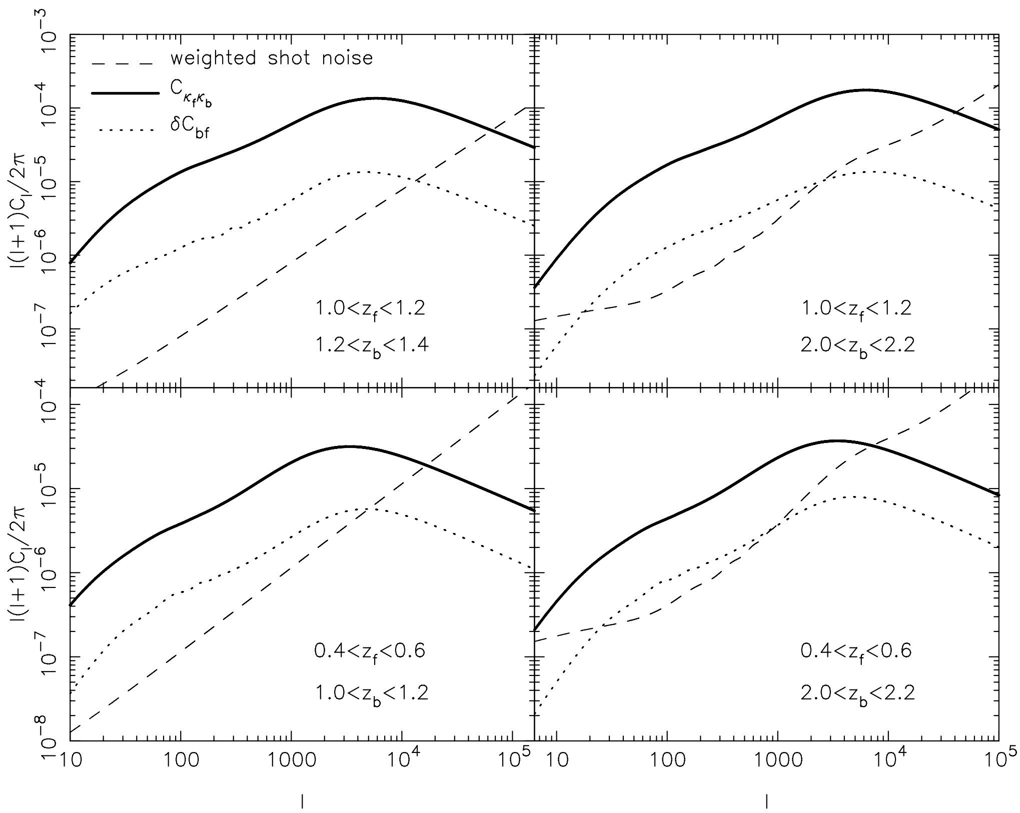

Figure 7. The weak lensing signal, the systematic error and the statistical error in the weak lensing reconstruction from the foreground and background redshift bins. The solid line is the cross-correlation power spectrum of cosmic convergence. The dotted line represents the systematic error combining three types $\delta C_{\rm bf} = \delta C_{\rm bf}^{(1)} + \delta C_{\rm bf}^{(2)} + \delta C_{\rm bf}{}^{(3)}$ and the dashed line corresponds to the weighted shot noise. In $\delta C_{\rm bf}$, $\delta C_{\rm bf}^{(1)}$ from the deterministic galaxy bias is dominant and the systematic error from the stochastic bias can be avoided in such a cross-lensing power spectrum, namely $\delta C_{\rm bf}^{(2)} = 0$. For every pair of foreground and background redshift bins, the cross-reconstructed weak lensing signal dominates at the scale range $10 \lesssim \ell \lesssim 10^4$ and it can be measured to reach ∼10–20 per cent accuracy.

5 CONCLUSIONS AND DISCUSSIONS

We propose a minimal variance estimator to reconstruct the weak lensing convergence κ field through the cosmic magnification effect in the observed galaxy number density distribution. This estimator separates the galaxy intrinsic clustering from the lensing signal due to their distinctive dependences on the galaxy flux. Using SKA as an example, we demonstrate the applicability of our method, under highly simplified conditions. It is indeed able to significantly reduce systematic errors. We have identified and quantified residual systematic errors and found them in general under control. Extensive efforts will be made in future to test our reconstruction method more robustly and to improve this method.

Compared to previous works, our method has several key features/advantages.

(i) Unlike weak lensing reconstruction through cosmic shear, it does not involve galaxy shape measurement and reconstruction and hence avoids all potential problems associated with galaxy shapes. Hence the reconstructed lensing maps provide useful independent check against cosmic shear measurement.

(ii) Unlike existing cosmic magnification measurements which actually measure the galaxy–lensing cross-correlation, our estimator allows direct reconstruction of the weak lensing κ field. From the reconstructed κ, we are able to directly measure the lensing power spectra of the same source redshift bin and between two redshift bins. These statistics do not involve galaxy bias, making them more robust cosmological probes. The usual lensing tomography is also directly applicable.

(iii) Unlike our previous works (Zhang & Pen 2005, 2006), the new method does not require priors on the galaxy bias, especially its flux dependence. In using our method to measure the galaxy bias and the lensing signal, we do not adopt any priors on the galaxy bias (other than that it is deterministic) and treat the galaxy bias as a free function of scale and flux. The price to pay is the degradation in constraining the galaxy bias and in lensing reconstruction. Adding priors on the galaxy bias can further improve the reconstruction precision, although the reconstruction accuracy will be affected by uncertainties/biases in the galaxy bias prior. For this reason, we do not attempt to add priors on galaxy bias in the reconstruction.

(iv) Our method is complementary to a recent proposal made by Heavens & Joachimi (2011) of a nulling technique to reduce the galaxy intrinsic clustering by proper weighting in redshift. Compared to this method, our method only utilizes the extra information encoded in the flux dependence to reduce/remove the galaxy intrinsic clustering. It keeps the cosmological information encoded in the redshift dependence disentangled from the process of removing the intrinsic clustering.

The proposed approach is not the only way for weak lensing reconstruction through cosmic magnification. The current paper focuses on direct reconstruction of the lensing convergence κ map. In a companion paper, we will focus on direct reconstruction of the lensing power spectrum (Yang & Zhang, in preparation). We will show that by combining two-point correlation measurements between all the flux bins, the lensing power spectrum can be reconstructed free of assumptions on the galaxy intrinsic clustering. We will see that this approach is more straightforward, more consistent and easier to carry out. However, the method presented in this paper does have advantages. Since it reconstructs the lensing κ map, higher order lensing statistics such as the bispectrum can be measured straightforwardly. Furthermore, the reconstructed κ map can be straightforwardly correlated with other tracers of the large-scale structure. For example, it can be correlated with the lensing map reconstructed from cosmic microwave background (CMB) lensing (Seljak & Zaldarriaga 1999; Hu & Okamoto 2002) or 21-cm lensing. Furthermore, through this approach we can have a better understanding of the origin of various systematic errors, which can be entangled in the alternative approach.

Our reconstruction method is versatile to include other components of fluctuation in the galaxy number density. The extinction-induced fluctuation discussed earlier is one; high-order corrections to the cosmic magnification are another. Taylor expanding equation (1) to the second order, we obtain

$$\begin{aligned}\delta_g^L &= \delta_g + 2(\alpha-1)\kappa \\ &\quad + 2(\alpha-1)\left[(\kappa\delta_g - \langle\kappa\delta_g\rangle) + \frac{1}{2}(\gamma^2 - \langle\gamma^2\rangle)\right] \\ &\quad + (1-5\alpha+2g_2)[\kappa^2 - \langle\kappa^2\rangle] + O[\kappa^3, \gamma^3, \ldots]. \end{aligned} \tag{32}$$

Here $g_2 \equiv (s^2/n)\mathrm{d}^2n/\mathrm{d}s^2$ is related to the second derivative of the luminosity function.

The above result shows that the κ reconstruction through cosmic magnification is biased by terms proportional to $\kappa\delta_g$ and γ^2 (second line in the above equation). Similar biases also exist in cosmic shear measurement. We recognize $\kappa\delta_g$ as the source–lens coupling. The γ^2 term is analogous to the $\kappa\gamma$ term caused by reduced shear $\gamma/(1-\kappa)$. Precision lensing cosmology has to model these corrections appropriately.

The high-order corrections $\propto 1 - 5\alpha + 2g_2$ can in principle be separated due to their unique flux dependence. However, it is unclear whether the reconstruction is doable, even for a survey as advanced as SKA.

ACKNOWLEDGMENTS

This work is supported by the One-Hundred Talents programme of the Chinese Academy of Sciences, the National Science Foundation of China (grant No. 10821302, 10973027, 11025316 and 10973018), the CAS/SAFEA International Partnership Program for Creative Research Teams and the National Basic Research Program of China (973 Program) under grant No.2009CB24901.

REFERENCES

Abdalla F. B., Rawlings S., 2005, MNRAS, 360, 27
Abdalla F. B., Blake C., Rawlings S., 2010, MNRAS, 401, 743
Albrecht A. et al., 2006, preprint (arXiv:astro-ph/0609591)
Bacon D. J., Refregier A. R., Ellis R. S., 2000, MNRAS, 318, 625
Choudhury T. R., Padmanabhan T., 2002, ApJ, 574, 59
Croft R. A. C., Metzler C. A., 2000, ApJ, 545, 561
Dekel A., Lahav O., 1999, ApJ, 520, 24
Dewdney P. E., Hall P. J., Schilizzi R. T., Lazio T. J. L. W., 2009, IEEE Proc., 97, 1482
Fan Z., 2003, ApJ, 594, 33
Faulkner A. J. et al., 2010, SKADS Memos: http://www.skads-eu.org
Fu L. et al., 2008, A&A, 479, 9
Gil-Marin H., Wagner C., Verde L., Jimenez R., Heavens A. F., 2010, MNRAS, 407, 772
Heavens A. F., Benjamin J., 2011, preprint (arXiv:1101.3337)
Heavens A., Refregier A., Heymans C., 2000, MNRAS, 319, 649
Heymans B. et al., 2006, MNRAS, 368, 1323
Hildebrandt H., Van Waerbeke L., Erben T., 2009, A&A, 507, 683
Hirata C. M., Seljak U., 2004, Phys. Rev. D, 70, 063526
Hirata C. M., Mandelbaum R., Ishak M., Seljak U., Nichol R., Pimbblet K. A., Ross N. P., Wake D., 2007, MNRAS, 381, 1197
Hoekstra H., Jain B., 2008, Annu. Rev. Nuclear Part. Syst., 58, 99
Hoekstra H., Van Waerbeke L., Gladders M. D., Mellier Y., Yee H. K. C., 2002, ApJ, 577, 604
Hu W., Okamoto T., 2002, ApJ, 574, 566
Jing Y. P., 1998, ApJ, 503, L9
Jing Y. P., 2002, MNRAS, 335, L89
Jing Y. P., Zhang P., Lin W. P., Gao L., Springel V., 2006, ApJ, 640, L119
Kaiser N., Wilson G., Luppino G. A., 2000, preprint (arXiv:astro-ph/0003338)
Komatsu E. et al., 2009, ApJS, 180, 330
Mandelbaum R., Hirate C. M., Ishak M., Seljak U., Brinkmann J., 2006, MNRAS, 367, 611
Massey R. et al., 2007, MNRAS, 376, 13
Menard B., 2002, preprint (arXiv:astro-ph/0210142)
Menard B., Scranton R., Fukugita M., Richards G., 2010, MNRAS, 405, 1025
Munshi D., Valageas P., van Waerbeke L., Heavens A., 2008, Phys. Rep., 462, 67
Okumura T., Jing Y. P., 2009, ApJ, 694, L83
Okumura T., Jing Y. P., Li C., 2009, ApJ, 694, 214
Pen U.-L., 1998, ApJ, 504, 601
Pen U.-L., 2004, MNRAS, 350, 1445
Pen U.-L., Lu T., Van Waerbeke L., Mellier Y., 2003, MNRAS, 346, 994
Peroux C., Irwin M. J., McMahon R. G., Storrie-Lombardi L. J., 2001, Ap&SS, 277, 551
Peroux C., McMahon R. G., Storrie-Lombardi L. J., Irwin M. J., 2003, MNRAS, 346, 1103
Peroux C., Deharveng J. M., Brun V. L., Cristiani S., 2004, MNRAS, 352, 1291
Refregier A., 2003, ARA&A, 41, 645
Rudd D. H., Zentner A. R., Kravtsov A. V., 2008, ApJ, 672, 19
Scranton R. et al., 2005, ApJ, 633, 589
Seljak U., Zaldarriaga M., 1999, Phys. Rev. Lett., 82, 2636
Swanson M. E. C., Tegmark M., Blanton M., Zehavi I., 2008, MNRAS, 385, 1635
Van Waerbeke L., 2010, MNRAS, 401, 2093
Van Waerbeke L. et al., 2000, A&A, 358, 30
Wang Y., Yang X., Mo H. J., Van den Bosch F. C., 2007, ApJ, 664, 608
White M., 2004, Astropart. Phys., 22, 211
Wittman D. M., Tyson J. A., Kirkman D., Dell'Antonio I., Bernstein G., 2000, Nat, 405, 143
Zhan H., Knox L., 2004, ApJ, 616, L75
Zhang P. J., Pen U.-L., 2005, Phys. Rev. Lett., 95, 241302
Zhang P. J., Pen U.-L., 2006, MNRAS, 367, 169
Zwaan M. A. et al., 2003, AJ, 125, 2842

APPENDIX A: SKA SURVEY

SKA is a future radio survey aiming to construct the world's largest radio telescope. Through the neutral hydrogen-emitting 21-cm hyperfine transition line, it can observe large samples of 21-cm galaxies. Even at high redshift, the observed 21-cm galaxies are in extreme excess of the QSOs or LBGs that are usually used as background objects (Scranton et al. 2005; Hildebrandt et al. 2009), so it is easy to overcome the problem of shot noise sensitivity of the measurement of the cosmic magnification effect. In addition, compared to a photometric survey, the spectroscopic survey can determine the redshift more precisely by using the redshifted wavelength of the 21-cm line [$\lambda = \lambda_0(1 + z)$]. Furthermore, a radio survey is free of galactic dust extinction, which is correlated with foreground galaxies and then induces a correction to the galaxy–galaxy cross-correlation. As a consequence, our proposed method is expected to give a good performance in measuring the cosmic magnification for SKA. In this paper, we adopt the survey specifications as follows: the telescope FOV is $10\,\mathrm{deg}^2$ without evolution, the overall survey time is 5 yr and the sky coverage is $10\,000\,\mathrm{deg}^2$.

A1 H I mass limit

By assuming a flat profile for the emission line with frequency, we obtain the following equation linking $M_{\mathrm{H\,I}}$ with the observed flux density s by atomic physics (details are given in Abdalla & Rawlings 2005):

$$M_{\mathrm{H\,I}} = \frac{16\pi}{3}\frac{m_{\mathrm{H}}}{A_{21}hc}\chi^2(z) s V(z)(1+z), \tag{A1}$$

where $\chi(z)$ is the comoving angular distance, A_{21} is spontaneous transition rate, m_{H} is the atomic mass of hydrogen, h is the Planck constant and $V(z)$ is the line-of-sight velocity spread. We assume a scaling with redshift for the typical rest-frame velocity width of the line $V(z) = V_0/\sqrt{1+z}$, where $V_0 = 300\,\mathrm{km\,s^{-1}}$, and ignore the effects of inclination. The rms sensitivity for a dual-polarization radio receiver at system temperature T_{sys} for an integration of duration t on a telescope of effective collecting area A_{eff} is given by

$$s_{\mathrm{rms}} = \frac{\sqrt{2}T_{\mathrm{sys}}}{\eta_{\mathrm{c}} A_{\mathrm{eff}}}\frac{k_B}{\sqrt{\Delta\nu t}}. \tag{A2}$$

Here, the correlation efficiency η_{c} is adopted as $\eta_{\mathrm{c}} = 0.9$, the duration time $t = 40$ h for each area of the sky and the width of the H I emission line determines the relevant frequency bandwidth $\Delta\nu$, which is related to a line-of-sight velocity width $V(z)$ at redshift z:

$$\Delta\nu = \frac{\nu_0}{1+z}\frac{V(z)}{c}. \tag{A3}$$

The flux detection limit s_{lim} for galaxies is defined by the threshold parameter $n_\sigma = s_{\mathrm{lim}}/s_{\mathrm{rms}}$. Here, we apply $n_\sigma = 5$. From equation (A1), we can obtain the H I mass limit.

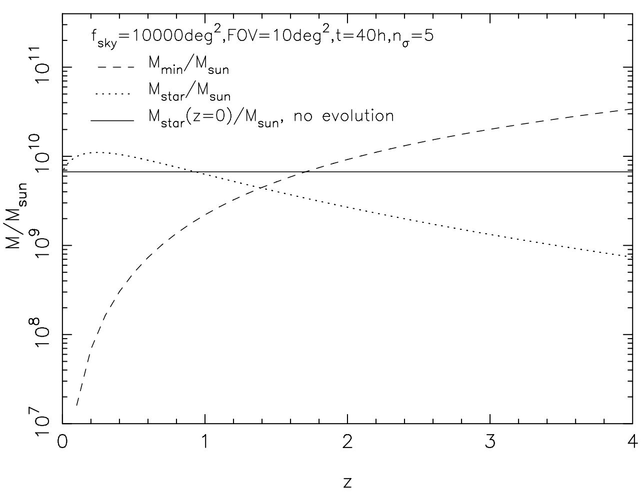

Figure A1. The redshift evolutions of H I mass limit (dashed line) and the characteristic mass in model C (dotted line). The characteristic mass in the no-evolution model is plotted by the solid line.

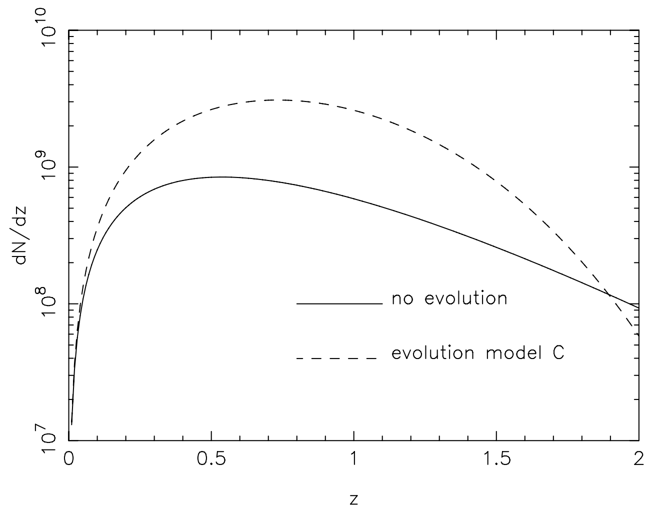

Figure A2. The redshift distributions of H I galaxies for the no-evolution model and evolution model C.

A2 H I mass function

We assume that the H I mass function at all redshifts is described by a Schechter function,

$$\phi(M_{\mathrm{H\,I}}, z)\mathrm{d}M_{\mathrm{H\,I}} = \phi^*\left(\frac{M_{\mathrm{H\,I}}}{M^*}\right)^\beta \exp\left(-\frac{M_{\mathrm{H\,I}}}{M^*}\right)\frac{\mathrm{d}M_{\mathrm{H\,I}}}{M^*}. \tag{A4}$$

Here, the parameter β is low-mass slope, M^* is characteristic mass and ϕ^* is normalization. The HIPASS survey reported the following results: $\beta = -1.3$, $M^*(z=0) = 3.47\,h^{-2}10^9\,\mathrm{M_\odot}$ and $\phi^* = 0.0204\,h^3\,\mathrm{Mpc}^{-3}$ (Zwaan et al. 2003). There is little robust measurement of $\phi^*(z)$ and $M^*(z)$ other than in the local Universe. But for this form of the mass function, there exists a tight relation between $\Omega_{\mathrm{H\,I}}$, the present-day critical density $\rho_{\mathrm{c}}(z=0)$ and $\phi^*(z)M^*(z)$:

$$\Omega_{\mathrm{H\,I}}h = \Gamma(\beta+2)\phi^* M^*(z)/\rho_{\mathrm{c}}(z=0), \tag{A5}$$

where Γ is the Gamma function. Observation of damped Lyman α (DLA) systems and Lyman α limit systems can be used to measure $\Omega_{\mathrm{H\,I}}$ (Peroux et al. 2001, 2003, 2004). We use the following functional form produced by fitting to DLA data points used in the paper by Abdalla et al. (2010):

$$\Omega_{\mathrm{H\,I}} = N\left[1.813 - 1.473(1+z)^{-2.31}\right]. \tag{A6}$$

The normalization constant N is fixed by the value of $\phi^*(z=0)M^*(z=0)$.

Here, we adopt model C from Abdalla & Rawlings (2005) and Abdalla et al. (2010) as the H I mass function evolution model. In this model, ϕ^* scales with z by using the DLA results. The break in the mass function M^* is controlled by the cosmic star formation rate and is given by

$$\frac{M^*(z)}{M^*(0)} = \left(\frac{\Omega_{\mathrm{star}}(0)/\Omega_{\mathrm{H\,I}}(0)+2}{\Omega_{\mathrm{star}}(z)/\Omega_{\mathrm{H\,I}}(z)+2}\right)D^3(z), \tag{A7}$$

where it is assumed that $\Omega_{\mathrm{H\,I}}(z) = \Omega_{\mathrm{H_2}}(z)$ and $D(z)$ is the growth factor. The fractional density in stars $\Omega_{\mathrm{star}}(z) = \rho_{\mathrm{star}}(z)/\rho_{\mathrm{c}}(z=0)$ is deduced by using the fits to the cosmic star-formation history in Choudhury & Padmanabhan (2002):

$$\Omega_{\mathrm{star}}(z) = \frac{1}{\rho_{\mathrm{c}}(z=0)}\int_z^\infty \frac{\mathrm{SFR}(z')}{H(z')(1+z')}\mathrm{d}z' \tag{A8}$$

and

$$\mathrm{SFR}(z) = \frac{0.13}{1+6\exp(-2.2z)}\left(\frac{h}{0.5}\right)\left(\frac{1}{2.5}\right)\frac{\chi_{\mathrm{fid}}(z)}{\chi(z)}. \tag{A9}$$

Here, $\chi(z)$ and $\chi_{\mathrm{fid}}(z)$ are the comoving distances at redshift z for the adopted cosmology model and a fiducial cosmology model with $\Omega_{\mathrm{M}} = 1$ and $\Omega_\Lambda = 0$, respectively. The unit of SFR is $h^2\,\mathrm{M}_\odot\,\mathrm{yr}^{-1}\,\mathrm{Mpc}^{-3}$. Fig. A1 shows the evolutions of H I mass limit and characteristic mass in evolution model C. The no-evolution characteristic mass is also plotted for comparison. In Fig. A2, we plot the redshift distributions of H I galaxies for the evolution model C and the no-evolution model.

A3 The slope of the H I galaxy number count

In equation (5), n is the mass function of H I galaxies. We can derive the parameter α as a function of flux s and redshift z, which is

$$\alpha(M_{\mathrm{HI}}, z) = -\beta - 1 + \frac{M_{\mathrm{HI}}}{M^*(z)} = \alpha(s, z). \tag{A10}$$

The relationship between flux s and M_{HI} is given by equation (A1).

A4 The galaxy bias b_{g} for H I galaxies

In our forecast, we adopt a deterministic bias b by assuming the cross-correlation coefficient $r = 1$, and hence we estimate the error induced by this assumption.

The large-scale bias of H I galaxies has been estimated by the method presented in Jing (1998):

$$b(M_{\mathrm{DM}}, z) = \left(\frac{0.5}{\nu^4} + 1\right)^{(0.06-0.02n_{\mathrm{eff}})}\left(1 + \frac{\nu^2-1}{\delta_{\mathrm{c}}}\right), \tag{A11}$$

where $\nu = \delta_{\mathrm{c}}(z)/\sigma(M_{\mathrm{DM}})$. $\sigma(M_{\mathrm{DM}})$ is the linearly evolved rms density fluctuation with a top-hat window function and $\delta_{\mathrm{c}}(z) = 1.686/D(z)$. The effective index is defined as the slope of $P(k)$ at the halo mass M_{DM}:

$$n_{\mathrm{eff}} = \frac{\mathrm{d}\ln P(k)}{\mathrm{d}\ln k}\Big|_{k=\frac{2\pi}{R}}; \qquad R = \left(\frac{3M_{\mathrm{DM}}}{4\pi\rho_{\mathrm{c}}(0)}\right)^{1/3}. \tag{A12}$$

H I galaxies are selected by their neutral hydrogen mass M_{HI}. To calculate the associated biases of these galaxies, we need to convert M_{HI} to the galaxy total mass M_{DM}. Since most baryons and dark matter are not in galaxies while most neutral hydrogen atoms are in galaxies, we expect that $f_{\mathrm{HI}} \gg \Omega_{\mathrm{HI}}/\Omega_{\mathrm{m}}$. Here, we choose $f_{\mathrm{HI}} = 0.1$. Although there are some problems in modelling the H I galaxy bias in this way, we emphasize that our reconstruction method is not limited to the specific values of the adopted galaxy bias, as long as the galaxy bias has a flux dependence different from the magnification bias. Their different flux dependences are presented in Fig. 3.

This paper has been typeset from a TEX/LATEX file prepared by the author.